

3.6 三次元走時表を用いた震源決定

本項の論文は、SSA（アメリカ地震学会）のオープンアクセス指針に従った上で掲載している。

(Katsumata, A., 2015: Fast hypocenter determination in an inhomogeneous velocity structure using a 3D travel-time table, *Bull. Seismol. Soc. Am.*, **105**, 3203–3208, doi:10.1785/0120150122)

Bulletin of the Seismological Society of America

This copy is for distribution only by
the authors of the article and their institutions
in accordance with the Open Access Policy of the
Seismological Society of America.

For more information see the publications section
of the SSA website at www.seismosoc.org



THE SEISMOLOGICAL SOCIETY OF AMERICA
400 Evelyn Ave., Suite 201
Albany, CA 94706-1375
(510) 525-5474; FAX (510) 525-7204
www.seismosoc.org

Short Note

Fast Hypocenter Determination in an Inhomogeneous Velocity Structure Using a 3D Travel-Time Table

by Akio Katsumata

Abstract The computer processing time required for raytracing and hypocenter determination in a 3D inhomogeneous velocity structure is too great for the method to be used to locate a large number of hypocenters or for interactive processing. In this study, hypocenter determinations were conducted using 3D travel-time tables (3D-TTs) to reflect travel times of a 3D inhomogeneous velocity structure in event locations, and the results were compared with those achieved using the 3D raytracing method. The use of 3D-TTs reduced the calculation time by a factor of about 1800 compared with the raytracing method. Whereas minor differences between interpolated travel times and the raytracing method caused some corresponding location differences, the travel-time table was effective for correction of hypocenter locations according to an inhomogeneous velocity-structure model.

Introduction

1D velocity structures have commonly been used to calculate hypocenters. In complex tectonic settings such as the Japanese Islands, the inhomogeneity of the velocity structure considerably reduces the accuracy of hypocenter locations. Location errors due to inadequate velocity structure models have been acknowledged since the early days of numerical hypocenter determinations (e.g., [Ichikawa, 1979](#)).

Efforts have since been made to improve the accuracy of hypocenter distributions determined in areas of inhomogeneous velocity structure. For earthquakes near the Kuril Islands, [Ichikawa \(1979\)](#) introduced a travel-time table, which was different from that for averaged Japanese islands structure, to deal with offsets between hypocenters derived from a local network and those derived from global networks. Several studies have shown that station corrections can provide an effective method to deal with shallow velocity differences. For example, the joint hypocenter determination method ([Douglas, 1967](#)) was developed to obtain adjustment functions for individual stations. [Hurukawa and Ohmi \(1993\)](#) used station corrections expressed as a quadratic function of hypocenter coordinates to determine hypocenters. [Richards-Dinger and Shearer \(2000\)](#) used source-specific station terms obtained by smoothing the residuals from nearby events. [Waldhauser and Ellsworth \(2000\)](#) developed a double-difference algorithm for earthquake location, which reduced the residuals between the observed and predicted phase travel-time differences for pairs of earthquakes recorded at common stations; this approach provided high-resolution hypocenter distributions.

Investigations of velocity structure, such as tomographic analysis, can provide high-resolution regional and global veloc-

ity models that improve the relative and absolute locations of hypocenters (e.g., [Aki and Lee, 1976](#); [Koch, 1985](#); [Johnson and Vincent, 2002](#); [Murphy et al., 2005](#); [Flanagan et al., 2007](#)). To locate seismic events within a 3D velocity structure, it is necessary to calculate travel times for individual stations, which requires considerable central processing unit (CPU) time. The finite-difference approximation (e.g., [Hole and Zelt, 1995](#)) has been used to calculate travel times at grid points in 3D velocity models ([Johnson and Vincent, 2002](#); [Flanagan et al., 2007](#)). [Ritzwoller et al. \(2003\)](#) used a modified 2D raytracer to calculate travel times for a 3D velocity model. [Myers et al. \(2010\)](#) developed a fast method of travel-time calculation for inhomogeneous velocity models that is suitable for use in routine seismic analysis without travel-time lookup tables.

Despite the above technological advances, calculation time remains a problem for hypocenter determination within a 3D velocity structure. This article evaluates calculation times for hypocenter determinations in a 3D inhomogeneous velocity structure by using travel-time lookup tables compiled by raytracing for each seismic station in Japan.

Velocity Structure

The velocity structure model used in this study was based on that obtained from tomographic analyses by [Katsumata \(2010\)](#), in which depth of the Moho beneath the Japanese Islands was estimated. However, discontinuities in that model were smoothed in this study to avoid gaps of hypocenter distribution caused by velocity steps. Velocity distributions were expressed as 3D B-spline functions ([Ichida and Yoshimoto, 1979](#)) corresponding to the summation of slowness ([Katsumata,](#)

Table 1
Grid Intervals for Travel-Time Tables

	$\Delta \leq 1^\circ$	$1^\circ < \Delta \leq 2^\circ$	$\Delta > 2^\circ$
$H \leq 50(\text{km})$	2', 2 km	4', 5 km	6', 5 km
$50(\text{km}) < H \leq 200(\text{km})$	4', 5 km	6', 10 km	6', 10 km
$H > 200(\text{km})$	6', 10 km	6', 10 km	6', 10 km

Longitude/latitude intervals and depth intervals are shown for various epicentral and focal-depth ranges. Δ and H denote epicentral distance and focal depth, respectively. The center of the top of each block is the reference point for Δ ranges.

2010) within the area bounded by latitudes 17° N and 53° N and longitudes 116° E and 158° E. The interval between knots of the B-spline function was one-sixth of a degree for depths shallower than 100 km and one-third of a degree for depths greater than 50 km. Slowness was linearly interpolated in the overlapped depth range of 50–100 km.

Travel-Time Table

Tables of 3D travel time based on the 3D velocity structure were prepared for each recording station. Travel times for individual stations were calculated at grid points in a 3D volume (as described below) by using the raytracing method of [Um and Thurber \(1987\)](#). Travel times (P - and S -wave first arrivals) were calculated for individual 3D blocks within which events had been detected. Two types of block were used, depending on distance from recording stations. In areas close (within 0.44° in the horizontal and 44 km in the vertical) to recording stations, a denser and inhomogeneous grid was used in which grid nodes were set at points where the distance from the station was proportional to the square of sequential number I from the station ($0.001 \times I^2$ degree in latitude and longitude; $0.1 \times I^2$ km in depth). This inhomogeneous grid was introduced to enhance grid density close to the station. For locations distant from recording stations, the blocks were set with constant grid intervals and dimensions of $1^\circ(\text{longitude}) \times 1^\circ(\text{latitude}) \times 50 \text{ km}(\text{depth})$. The grid intervals were set based on epicentral distance and focal depth (Table 1).

To take into account all events recorded at 1813 recording stations from the start of the unified seismic catalog in Japan in October 1997 ([Japan Meteorological Agency, 1998](#)) to August 2014, about 250,000 blocks were required and about 1.5 billion data points were generated. Processing these to produce travel-time tables consumed about 94,000 hrs of CPU time, which equates to about one month of elapsed time for 128-core ordinary cluster computing. The average CPU time required to trace one ray was 0.2 s. The total storage required for the travel-time tables was about 12 GB.

Interpolation of Travel-Time Table

Travel times were calculated by interpolating between grid values. Although forcing interpolated values to agree with values at grid points is preferable, to do so increases

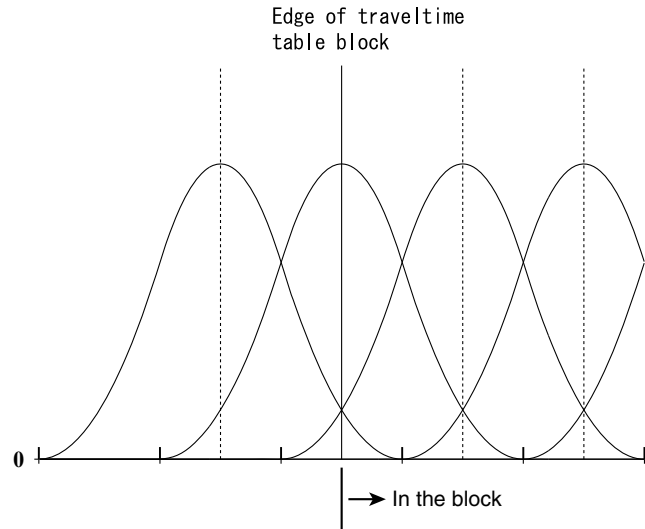


Figure 1. Knot positions of B-spline functions (ticks on baseline) and grid-point positions of travel-time table (vertical broken and solid lines). Knot positions are set so that the grid points are located at the peaks of B-spline functions.

processing time considerably if second-order or higher interpolation is used. Here, travel time was interpolated by multiplying the B-spline functions by the grid values as follows:

$$t(\lambda, \phi, h) = \sum_{i=1}^{p-m} \sum_{j=1}^{q-m} \sum_{k=1}^{r-m} t_{ijk} N_{mi}(\lambda) N_{mj}(\phi) N_{mk}(h), \quad (1)$$

in which $t(\lambda, \phi, h)$ is interpolated travel time at longitude (λ), latitude (ϕ), and depth (h), and t_{ijk} is the travel time at a grid point calculated by the raytracing method. $N_{mi}(\lambda)$, $N_{mj}(\phi)$, and $N_{mk}(h)$ are normalized B-spline functions of order $m - 1$, and p , q , and r are the number of knots for longitude, latitude, and depth, respectively. Second-order splines were used. If t_{ijk} are the same value, the summation of equation (1) makes a value identical to the constant. Spline knots were equidistant between grid points (Fig. 1). Where the grid interval in adjoining blocks was the same, there were no stepwise changes of interpolated values across the block boundaries. Interpolated values generally differed from grid values; these differences are covered in the [Travel-Time Difference Due to Interpolation](#) section.

For application in this study, the travel-time calculation subroutine of the hypocenter determination program used operationally by the Japan Meteorological Agency ([Hamada et al., 1983](#); [Ueno et al., 2002](#)) was replaced. Differential coefficients of travel times used for hypocenter determination were calculated by differentiating B-spline functions as follows:

$$\frac{\partial t(\lambda, \phi, h)}{\partial \lambda} = \sum_{i=1}^{p-m} \sum_{j=1}^{q-m} \sum_{k=1}^{r-m} t_{ijk} \frac{dN_{mi}(\lambda)}{d\lambda} N_{mj}(\phi) N_{mk}(h). \quad (2)$$

These differential coefficients do not show stepwise changes if second-order (or higher) spline functions are used. Blocks of

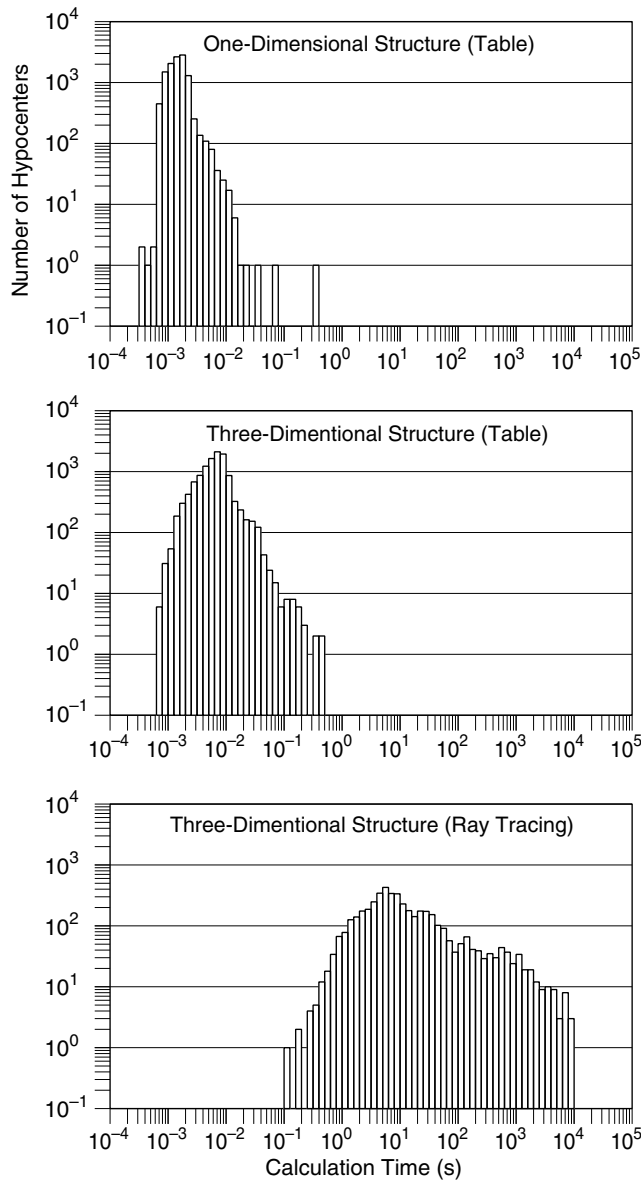


Figure 2. Distributions of calculation times for hypocenter determinations for the three methods considered in this study. The number of events in every 0.1 interval of $\log_{10} t_c$ is shown on the vertical axis, where t_c is a calculation time of an event.

travel-time data were dynamically loaded into memory during hypocenter calculation. The number of blocks per station in memory at any time was limited to two.

Calculation Time

Calculation times to locate 11,448 events (recorded in the unified seismic catalog for Japan in January 2014) were compared for determinations using a 1D-TT (Ueno *et al.*, 2002), 3D-TT, and the 3D raytracing method (3D-RT) (Fig. 2). Calculation times per event for 1D-TT and 3D-TT on an ordinary workstation were less than 1 s. The maximum calculation time for 3D-TT was short enough to be used in interactive

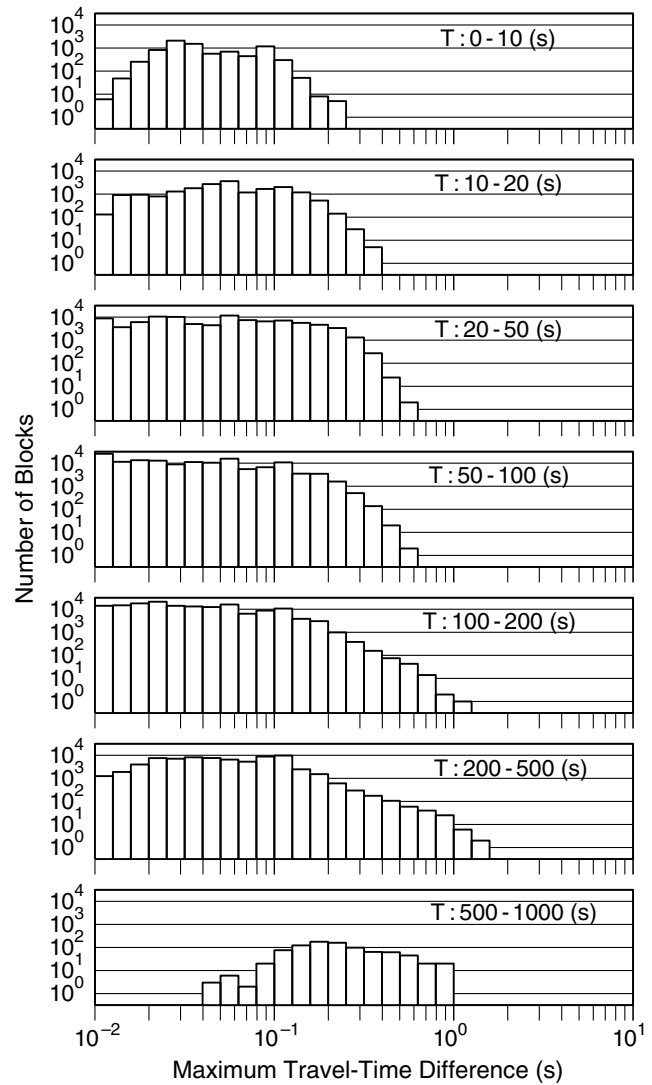


Figure 3. Distribution of maximum travel-time differences between grid-point values determined by raytracing and by interpolation according to equation (1) for various time intervals. The reference travel time T is that corresponding to the maximum travel-time difference in a block.

processing. Some calculation times for 3D-RT were nearly 10,000 s. Average logarithmic calculation times for 3D-TT were about 1800 times faster than those for 3D-RT. On the other hand, calculation times for 1D-TT were four times faster than those for 3D-TT.

Travel-Time Difference Due to Interpolation

Interpolated travel times at block grid points (equation 1) differed from those calculated by the raytracing method. The maximum travel-time differences for both P - and S -waves for every grid point in all blocks were less than 0.1 s for 82% of blocks (Fig. 3). However, there were maximum travel-time differences of more than 1 s in 0.01% of blocks.

Most of the large travel-time differences were caused by stepwise changes due to ray-path scattering in response to a

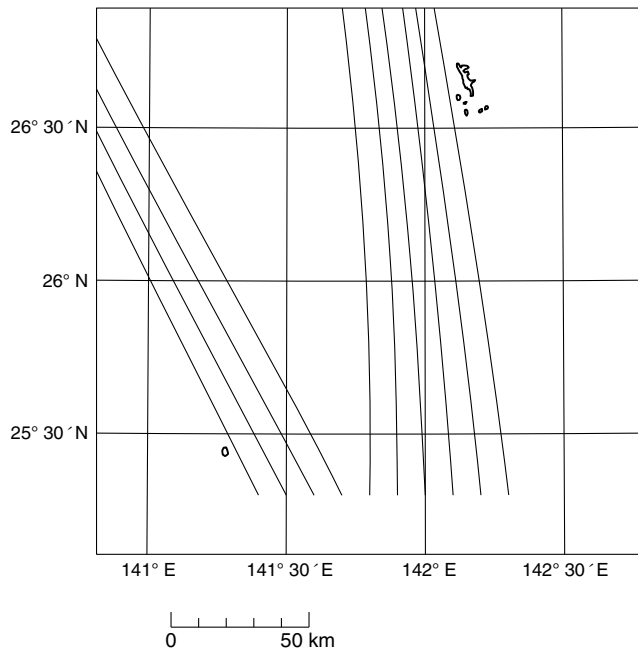


Figure 4. An example of ray paths showing stepwise travel-time change. The curves are ray paths from Matsushiro station (138°12.23'E, 36°32.75'N) to locations of 0.1° interval. A travel-time step appears when the ray path switches from westward bending to eastward bending.

velocity gradient. An example of ray-path scattering is shown in Figure 4. Small changes of hypocenter location can cause large ray-path differences and create stepwise changes of travel time. Testing various initial ray paths for raytracing allowed such stepwise variations to be reduced. However, for the example shown in Figure 4, testing of 15 initial ray paths failed to identify a ray path that removed considerable stepwise variations in the travel-time tables.

Location Difference Due to Interpolation

Hypocenter locations for events in January 2014 were compared for determinations by 1D-TT, 3D-TT, and 3D-RT (Fig. 5). “Distance ratios” (see caption of Fig. 5 for definition) were used for this comparison. A distance ratio greater than one indicates that a hypocenter determined by 3D-TT was closer to that determined by 1D-TT than it was to that determined by 3D-RT. Although the distance ratio was less than 1.0 for 98.3% of events, it approached 10 for some others. Many of the events with large distance ratios were offshore events or were inland events with small location differences. Comparison of travel-time differences of both 1D-TT and 3D-TT determinations with those of 3D-RT determinations for the events with largest difference ratios (Fig. 6) shows that, although the travel-time differences between 3D-TT and 3D-RT were small, the location differences were considerable. It is considered that these large difference ratios reflect unstable locating due to small residual travel-time differences according to location difference.

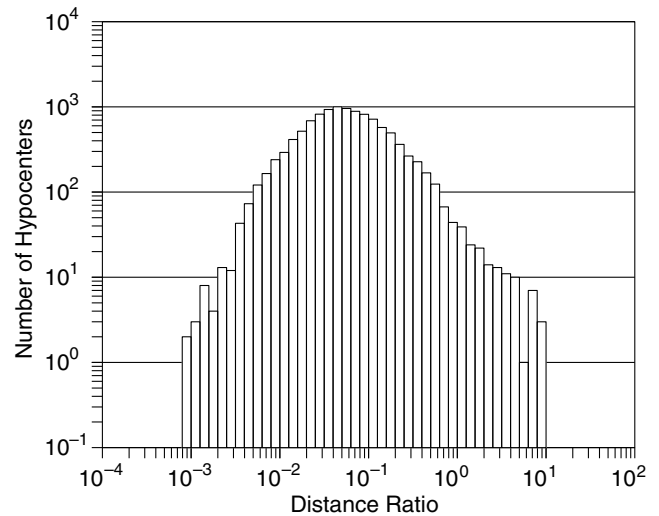


Figure 5. Comparison of differences of hypocenter locations determined by the 1D travel-time table (1D-TT), 3D travel-time table (3D-TT), and 3D raytracing method (3D-RT) methods. Distance ratio is defined as $D_{(3D-TT)-(3D-RT)} / D_{(1D-TT)-(3D-RT)}$, in which $D_{(3D-TT)-(3D-RT)}$ is the distance between the 3D-TT and 3D-RT locations and $D_{(1D-TT)-(3D-RT)}$ is the distance between 1D-TT and 3D-RT locations.

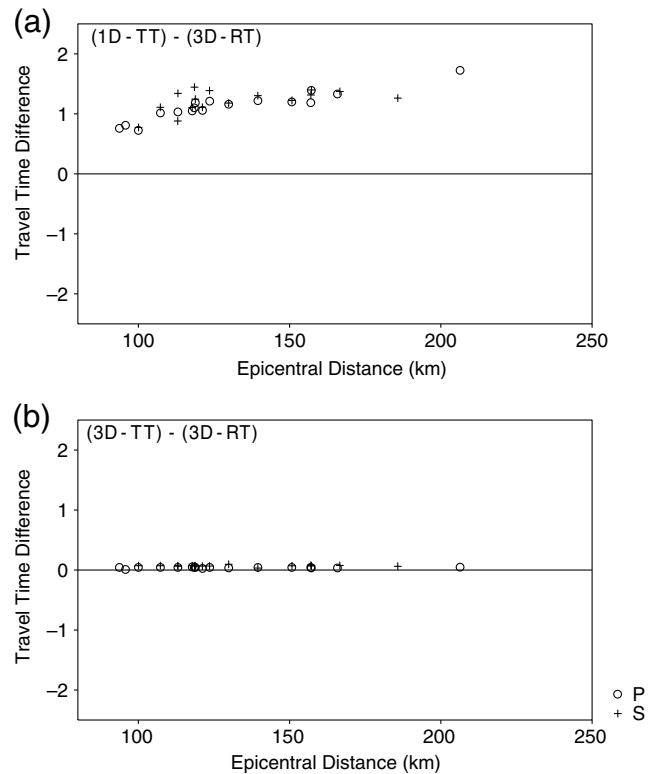


Figure 6. Travel-time difference between (a) 1D-TT and 3D-RT methods and (b) 3D-TT and 3D-RT methods for an event that showed the largest value of $D_{(3D-TT)-(3D-RT)} / D_{(1D-TT)-(3D-RT)}$. The reference hypocenter location is that determined by 3D-RT. The travel-time differences between 3D-TT and 3D-RT were slight even for the case of a large distance ratio.

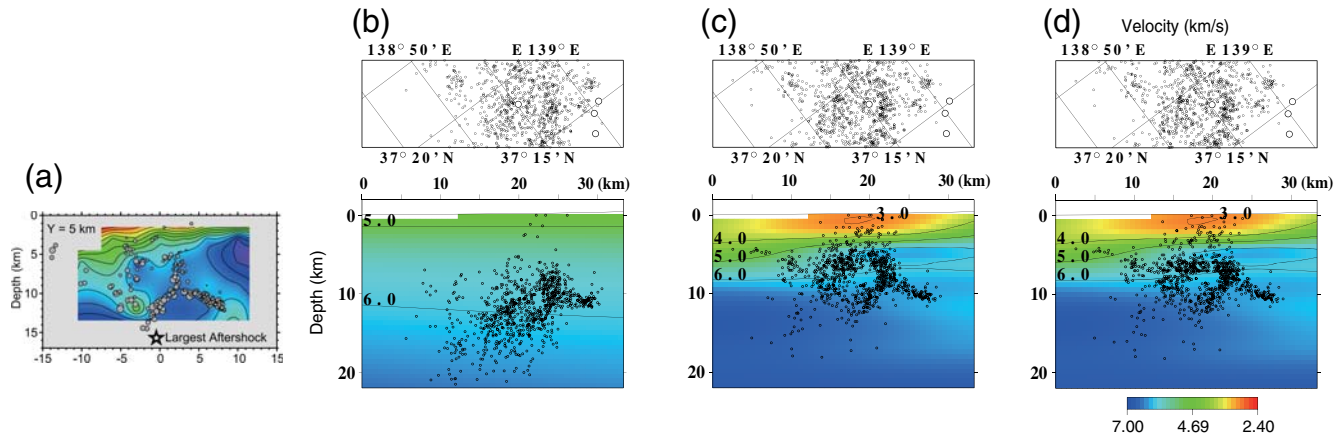


Figure 7. The comparison of hypocenter determinations for aftershocks of the 2004 Mid-Niigata Prefecture earthquake. Results of determinations (a) by Kato *et al.* (2005) with additional data from a temporarily deployed dense station network, (b) by the 1D-TT method, (c) by the 3D-TT method, and (d) by the 3D-RT method. For (b)–(d), epicenter distributions are shown in plan view in the upper panels and hypocenters in cross section in the lower panels. Black dots are epicenter and hypocenter locations, and open circles are locations of the recording stations. Aftershocks from 23 October 2004 to 31 December 2004 are included in (b)–(d). The color version of this figure is available only in the electronic edition.

The differences of hypocenter locations among 1D-TT, 3D-TT, and 3D-RT determinations are demonstrated by comparison of aftershock distributions determined by these methods for the Mid-Niigata Prefecture earthquake of 2004 (Fig. 7). The main difference for determinations using 1D-TT and 3D-TT is in the focal depths. Both the 3D-RT and 3D-TT methods provided shallower focal depths than the 1D-TT method. For both 3D methods, the aftershock distribution along the fault segment is clear and consistent with the results of Kato *et al.* (2005).

Conclusions

Calculation times were evaluated for hypocenter determinations using 3D-TTs to represent an inhomogeneous velocity structure and were compared with the calculation times achieved using 3D raytracing. The use of 3D-TTs shortened calculation time by a factor of about 1800, compared with the 3D-RT.

Interpolated travel times did not differ greatly from those calculated by raytracing. For some events, hypocenter locations from interpolated travel times differed notably from those calculated by raytracing. These differences were attributed to the combined effects of the travel-time differences and unstable locating due to small residual differences from location perturbation.

Data and Resources

We used seismic data from the National Research Institute for Earth Science and Disaster Prevention, Hokkaido University, Hirosaki University, Tohoku University, the University of Tokyo, Nagoya University, Kyoto University, Kochi University, Kyushu University, Kagoshima University, the National Institute of Advanced Industrial Science and Technology, the Tokyo metropolitan government, the Shizuoka

Prefectural government, the Kanagawa Prefectural government, the City of Yokohama, the Japan Marine Science and Technology Center, and the Japan Meteorological Agency.

Acknowledgments

We are grateful to anonymous reviewers and the editors for their thoughtful comments. Part of Figure 7 is reprinted with permission from John Wiley & Sons.

References

Aki, K., and W. H. K. Lee (1976). Determination of three-dimensional velocity anomalies under a seismic array using first *P* arrival times from local earthquakes: 1. A homogeneous initial model, *J. Geophys. Res.* **81**, 4381–4399, doi: [10.1029/JB081i023p04381](https://doi.org/10.1029/JB081i023p04381).

Douglas, A. (1967). Joint epicentre determination, *Nature* **215**, 47–48.

Flanagan, M. P., S. C. Myers, and K. D. Koper (2007). Regional travel-time uncertainty and seismic location improvement using a three-dimensional a priori velocity model, *Bull. Seismol. Soc. Am.* **97**, 804–825, doi: [10.1785/0120060079](https://doi.org/10.1785/0120060079).

Hamada, N., A. Yoshida, and H. Hashimoto (1983). Improvement of the hypocenter determination program of the Japan Meteorological Agency (reanalyses of the hypocenter distribution of the 1980 earthquake swarm off the east coast of the Izu Peninsula and the Matsushiro earthquake swarm), *Quarterly J. Seismol.* **48**, 35–55 (in Japanese with English abstract).

Hole, J. A., and B. C. Zelt (1995). 3-D finite difference reflection travel-times, *Geophys. J. Int.* **121**, 427–434.

Hurukawa, N., and S. Ohmi (1993). A hypocenter-determination method using station corrections as a function of hypocenter coordinates, *Zisin* **2** **46**, 285–295 (in Japanese with English abstract).

Ichida, K., and F. Yoshimoto (1979). *Spline Functions and Their Applications*, Kyoiku Shuppan, Tokyo, 220 pp. (in Japanese).

Ichikawa, S. (1979). Determination of hypocenters of earthquakes occurring off the east coast of northern Honshu, *Q. J. Seismol.* **43**, 59–65 (in Japanese with English abstract).

Japan Meteorological Agency (1998). *The Seismological and Volcanological Bulletin of Japan for October 1997*, Tokyo, 78 pp., http://www.data.jma.go.jp/svd/eqev/data/bulletin/index_e.html (last accessed September 2014).

- Johnson, M., and C. Vincent (2002). Development and testing of a 3D velocity model for improved event location: A case study for the India–Pakistan region, *Bull. Seismol. Soc. Am.* **92**, 2893–2910, doi: [10.1785/0120010111](https://doi.org/10.1785/0120010111).
- Kato, A., E. Kurashimo, N. Hirata, S. Sakai, T. Iwasaki, and T. Kanazawa (2005). Imaging the source region of the 2004 Mid-Niigata Prefecture earthquake and the evolution of a seismogenic thrust-related fold, *Geophys. Res. Lett.* **32**, L07307, doi: [10.1029/2005GL022366](https://doi.org/10.1029/2005GL022366).
- Katsumata, A. (2010). Depth of the Moho discontinuity beneath the Japanese Islands estimated by traveltimes analysis, *J. Geophys. Res.* **115**, no. B04303, doi: [10.1029/2008JB005864](https://doi.org/10.1029/2008JB005864).
- Koch, M. (1985). Nonlinear inversion of local seismic travel times for the simultaneous determination of the 3D-velocity structure and hypocentres—Application to the seismic zone Vrancea, *J. Geophys.* **56**, 160–173.
- Murphy, J. R., W. Rodi, M. Johnson, D. D. Sultanov, T. J. Bennett, M. N. Toksöz, V. Ovtchinnikov, B. W. Barker, D. T. Reiter, A. C. Rosca, *et al.* (2005). Calibration of International Monitoring System (IMS) stations in central and eastern Asia for improved seismic event location, *Bull. Seismol. Soc. Am.* **95**, no. 4, 1535–1560, doi: [10.1785/0120040087](https://doi.org/10.1785/0120040087).
- Myers, S. C., M. L. Begnaud, S. Ballard, M. E. Pasyanos, W. S. Phillips, A. L. Ramirez, M. S. Antolik, K. D. Hutchenson, J. J. Dwyer, C. A. Rowe, *et al.* (2010). A crust and upper-mantle model of Eurasia and North Africa for Pn travel-time calculation, *Bull. Seismol. Soc. Am.* **100**, no. 2, 640–656, doi: [10.1785/0120090198](https://doi.org/10.1785/0120090198).
- Richards-Dinger, K. B., and P. M. Shearer (2000). Earthquake locations in southern California obtained using source-specific station terms, *J. Geophys. Res.* **105**, no. B5, 10,939–10,960, doi: [10.1029/2000JB900014](https://doi.org/10.1029/2000JB900014).
- Ritzwoller, M. H., N. M. Shapiro, A. L. Levshin, E. A. Bergman, and E. R. Engdahl (2003). Ability of a global three-dimensional model to locate regional events, *J. Geophys. Res.* **108**, no. B7, 2353, doi: [10.1029/2002JB002167](https://doi.org/10.1029/2002JB002167).
- Ueno, H., S. Hatakeyama, T. Aketagawa, J. Funasaki, and N. Hamada (2002). Improvement of hypocenter determination procedures in the Japan Meteorological Agency, *Q. J. Seismol.* **65**, 123–134 (in Japanese with English abstract).
- Um, J., and C. Thurber (1987). A fast algorithm for two-point seismic ray tracing, *Bull. Seismol. Soc. Am.* **77**, 972–986.
- Waldhauser, F., and W. L. Ellsworth (2000). A double-difference earthquake location algorithm: Method and application to the northern Hayward fault, California, *Bull. Seismol. Soc. Am.* **90**, no. 6, 1353–1368, doi: [10.1785/0120000006](https://doi.org/10.1785/0120000006).

Meteorological Research Institute
Japan Meteorological Agency
Nagamine 1-1
Ibaraki Prefecture
Tsukuba 305-0052 Japan
akatsuma@mri-jma.go.jp

Manuscript received 29 September 2015;
Published Online 10 November 2015